PROCEEDINGS OF SPIE

SPIEDigitalLibrary.org/conference-proceedings-of-spie

Enhanced absorption sensing using non-adiabatic tapered fiber coupling to a whispering-gallery microresonator

Sreekul Raj Rajagopal, Limu Ke, A. T. Rosenberger

Sreekul Raj Rajagopal, Limu Ke, A. T. Rosenberger, "Enhanced absorption sensing using non-adiabatic tapered fiber coupling to a whispering-gallery microresonator," Proc. SPIE 10904, Laser Resonators, Microresonators, and Beam Control XXI, 109041D (4 March 2019); doi: 10.1117/12.2508024

SPIE.

Event: SPIE LASE, 2019, San Francisco, California, United States

Enhanced absorption sensing using non-adiabatic tapered fiber coupling to a whispering-gallery microresonator

Sreekul Raj Rajagopal, Limu Ke, and A. T. Rosenberger*
Department of Physics, Oklahoma State University, Stillwater, OK, USA 74078-3072

ABSTRACT

Adiabatically tapered fibers are often used to excite whispering gallery modes (WGMs) of microresonators used as chemical sensors. Recently it was demonstrated that using a non-adiabatic tapered fiber can enhance refractive index sensing. The incoming light is distributed between fundamental and higher-order fiber modes, whereas only the fundamental mode is detected because the uptaper is adiabatic. The interference effect between these fiber modes when exciting a WGM leads to the sensitivity enhancement. We have shown theoretically that even greater enhancement is possible for absorption sensing. For a given WGM, the predicted enhancement can be calculated by measuring the throughput power when the two fiber modes are in and out of phase at the input. Enhancement can be confirmed by sending the light in the reverse direction through the asymmetrically tapered fiber so that only one fiber mode is incident on the microresonator. Using a carefully designed asymmetrically tapered fiber, we have demonstrated this enhancement in experiments using a hollow bottle resonator (HBR) with an internal analyte. Absorption in the analyte causes a change in the WGM throughput fractional dip depth; these changes were studied with varying analyte concentration for forward and reverse propagation to evaluate the absorption sensitivity. For both liquid and gaseous analytes, our measured sensitivity enhancements are not inconsistent with the predicted enhancements of at least a factor of 100.

Keywords: microresonator, whispering-gallery modes, chemical sensing, non-adiabatic tapered fibers.

1. INTRODUCTION

Whispering gallery mode (WGM) microresonators have been studied in detail in recent decades. They have high quality factors and small mode volumes and hence have been widely used as optical sensors, offering high sensitivity. In practical applications, WGM microresonators have been used to monitor changes in pressure, temperature, chemical composition, refractive index, and other quantities.[1]

From the operational point of view, optical WGM sensors detect through the registration of changes in their spectral response due to perturbations in the surrounding environment. The most-used spectral features of a WGM are its resonance frequency and linewidth. The resonance frequency of a WGM shifts with a change in the refractive index of the surrounding medium, whereas different physical phenomena such as absorption and scattering can affect the linewidth of a WGM. Thus sensors based on resonance frequency and linewidth rely on changes in resonance frequency and linewidth, respectively, upon the interaction of a WGM with its surroundings. In addition to the change in linewidth, physical phenomena such as absorption can also induce a change in another spectral property, namely the resonant throughput dip depth, and thus absorption sensing can be studied in detail by monitoring the change in the dip depth of a WGM.

Previously it was demonstrated that absorption sensing based on dip depth change could provide better sensitivity than frequency shift measurements.[2] Experimental evidence[3] was provided by introducing trace gases into the surroundings of a cylindrical fused silica microresonator, and strain-tuning a WGM through a trace gas absorption line. The WGM's effective intrinsic loss gets modified and hence, on resonance with the trace gas absorption line, the dip depth changes by an amount that depends on the external evanescent fraction of the WGM interacting with its surroundings.

*atr@okstate.edu; phone 1 405 744-6742; fax 1 405 744-6811; physics.okstate.edu/rosenber/index.html

Laser Resonators, Microresonators, and Beam Control XXI, edited by Alexis V. Kudryashov, Alan H. Paxton, Vladimir S. Ilchenko, Proc. of SPIE Vol. 10904, 109041D · © 2019 SPIE
CCC code: 0277-786X/19/$18 · doi: 10.1117/12.2508024

The sensitivity of WGM sensors depends on the evanescent fraction of the mode. In addition to the external evanescent fraction, the internal evanescent fraction of a hollow microresonator can also be used for sensing purposes.[1,4] A microresonator such as a thin-walled hollow bottle resonator (HBR) offers internal evanescent fractions, which for some WGMs can be larger than their external evanescent fractions,[4,5] thereby improving the detection threshold. Previously we have demonstrated a simple and cost-effective way of making HBRs which permits their usage as internal evanescent wave WGM based optical absorption sensors.[6]

Recently a novel method for enhancing the sensitivity of evanescent wave WGM based optical absorption sensors was proposed.[7] Typically the WGMs of a microresonator are excited by coupling in tunable laser light using an adiabatically tapered fiber. The proposed scheme depends on using a non-adiabatic tapered fiber to couple light into the microresonators and under the right conditions the sensitivity can be enhanced as compared to using an adiabatic taper. In this paper, experimental proof for this enhancement in absorption sensing is provided.

2. HOLLOW BOTTLE RESONATOR AND MODE PROFILES

The hollow bottle resonator offers high quality factor, axial confinement of modes, mode selectivity, and strain-tunability. The hollow core of the HBR allows small volumes of the analyte to be sensed internally. The fabrication of a typical HBR[6] includes etching of a fused-silica capillary tube using a hydrofluoric acid solution to reduce the wall thickness to 5-10 μm and then a small portion of the etched capillary is heated while pressurizing to make a bulge.

Three indices and the polarization characterize a WGM in an HBR. The three indices are the azimuthal mode index which represents an integral number of wavelengths around the circumference, the radial index which represents the number of radial intensity maxima, and the axial index giving the number of axial field nodes. The HBR supports two orthogonally polarized families of modes, TE (transverse electric) and TM (transverse magnetic).

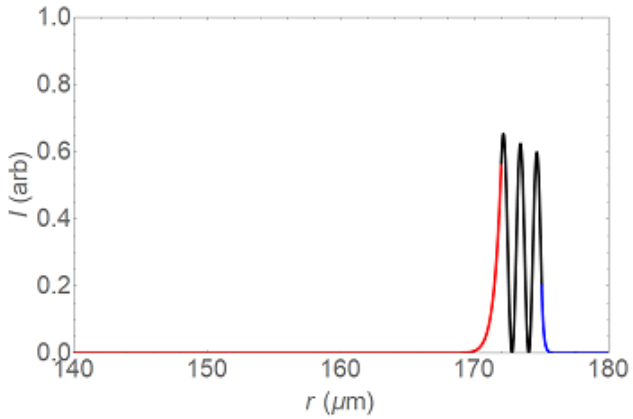

Fig. 1. TE mode profile of a WGM in an HBR with an outer boundary at 175 μm and inner boundary at 173 μm.

An example of the radial mode intensity profile of a WGM with water inside the resonator is shown in Fig. 1. The internal evanescent fraction (indicated by red) of the mode is much greater than the external (indicated by blue), and hence the HBR is highly recommended over other microresonators for internal sensing.

3. NON-ADIABATIC TAPERS

Adiabatic tapers[8] are commonly used to couple light into microresonators. A tapered fiber with an adiabatic taper transition will have light confined to a single mode of the taper waist, and thereby one fiber mode is incident on the microresonator. However, if the taper transition is non-adiabatic, multiple fiber modes can be excited, and hence more than one fiber mode can be incident on the microresonator, where they interfere while exciting a WGM of the microresonator.

A non-adiabatic tapered fiber is fabricated in our lab by using the conventional flame brush technique. A small portion of an optical fiber is stripped and attached to two motorized stages. Then the two stages are pulled at different speeds relative to each other. Meanwhile, the hydrogen flame continuously brushes over a fixed distance called the brushing length. The delineation curves plotted for the resulting tapered fiber suggest that the asymmetric tapered fiber has a non-adiabatic downtaper and an adiabatic uptaper. The schematic figure of an asymmetric taper is shown in Fig. 2. The radius of the untapered fiber is given by r_0, taper transition lengths on either side are z_1 and z_2, and L is the brushing length.

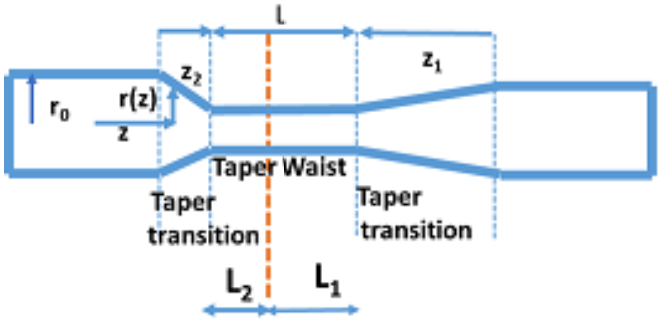

Fig. 2. An asymmetric tapered fiber with a non-adiabatic downtaper and an adiabatic uptaper.

Non-adiabatic tapered optical fibers can be used as sensors themselves. They have been used as refractive index sensors,[9] biosensors,[10] strain and temperature sensors,[11] and magnetic field sensors,[12] for example. For non-adiabatic tapered fibers, due to the large angle of the taper transition, multiple modes can be excited. These modes differ in their spatial profiles, refractive indices, evanescent fractions, and propagation constants. As the light propagates along the taper waist, the difference in propagation constants results in beating of the modes.

The throughput spectral profile of a resonator mode is a symmetric Lorentzian dip when an adiabatically tapered fiber is used to couple light into the microresonator. However, with a non-adiabatic tapered fiber, the dip gets asymmetric depending on the relative phase and amplitude of the fiber modes at the point of coupling to the microresonator. It was demonstrated that Fano resonances could be obtained and used for enhancement of frequency-shift sensing when the non-adiabatic tapered fiber is used to couple light into a microresonator.[13] Here we show that fiber mode interference at the point of HBR coupling acts, in turn, to enhance the absorption sensitivity.

4. MODEL AND THEORY

The effects of using a non-adiabatic tapered fiber to couple light into a microresonator can be explained by using a simple ring cavity model. The detailed explanation of the model is given in our previous work.[7] The numerical model depends on experimentally measured values such as the linewidth $\Delta\upsilon$, the HBR radius a, and the relative throughput when the fiber modes are in phase ($\beta = 0$) and out of phase ($\beta = \pi$).

Let E_{i1} and $E_{i2}e^{i\beta}$ be the amplitudes of the two fiber modes with a relative phase β at the point of coupling. T_1 and T_2 represent the strengths of coupling of the fiber modes to the WGM, and αL represents the intrinsic power loss per round trip.

The resonant throughput for forward propagation (non-adiabatic downtaper, adiabatic uptaper), $R(0)$, is given by

$$R(0) = \frac{(T_1 - T_2 - \alpha L)^2 + 4T_1T_2m^2 + 4(T_1 - T_2 - \alpha L)\sqrt{T_1T_2}\,m\cos\beta}{(T_1 + T_2 + \alpha L)^2}, \quad (1)$$

where m represents the ratio of amplitude moduli of the incident fiber modes. When $m = 0$, one fiber mode is incident on the microresonator, and hence the throughput profile is a symmetric Lorentzian dip. However, if $m > 0$, depending

on the values of other parameters, a symmetric peak or dip is obtained at $\beta = \pi$ or $\beta = 0$ respectively as shown in Fig. 3. The relative dip depth M is given by

$$M = \frac{4T_1(T_2 + \alpha L) - 4T_1T_2m^2 - 4(T_1 - T_2 - \alpha L)\sqrt{T_1T_2}\, m\cos\beta}{(T_1 + T_2 + \alpha L)^2}. \tag{2}$$

In order to calculate the dip depth change for absorption sensing, one needs to make three measurements with just the solvent inside the resonator: the throughput power corresponding to $\beta = \pi$ and $\beta = 0$, and the linewidth of the mode, $\Delta\upsilon$. From these three measurements, T_1, $T_2 + \alpha L$, and $T_1T_2m^2$ can be determined, and hence the dip depth changes can be calculated.

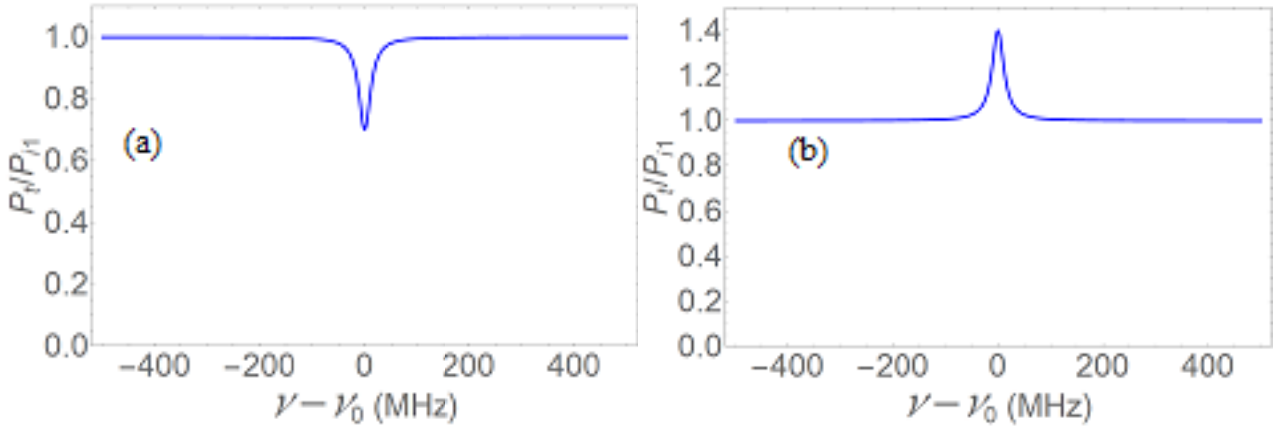

Fig. 3. Calculated throughput mode profiles corresponding to different relative fiber mode phase. (a) $\beta = 0$. (b) $\beta = \pi$.

Upon introducing analyte into the microresonator, the total loss αL becomes

$$\alpha L = \alpha_i L + f\alpha_s L + f\alpha_a L, \tag{3}$$

where $\alpha_i L$ is the intrinsic loss, α_s and α_a represent the absorption coefficients of solvent and analyte respectively, and f is the internal evanescent fraction of the mode. Knowing the value of α_a allows determination of f by fitting calculated dip depth to experimental dip depth, thus providing a way of comparing experimental results with predicted results for various analyte concentrations. Thus the fractional change in dip depth, $\frac{\Delta M}{M}$, for different analyte concentrations can be calculated and compared to the experiment.

With one fiber mode incident on the microresonator, i.e., $m = 0$, the fractional change in dip depth $\frac{dM}{M}$, will be small and is given by

$$\frac{dM}{M} = \frac{T_1 - T_2 - \alpha L}{(T_1 + T_2 + \alpha L)(T_2 + \alpha L)} d(\alpha L). \tag{4}$$

Thus the theoretical enhancement can be calculated by taking the ratio of $\frac{\Delta M}{M}$ to $\frac{dM}{M}$. The above equation assumes that a symmetric tapered fiber with adiabatic down- and uptapers is used to couple light into and out of the microresonator. If the direction of propagation of light through an asymmetric tapered fiber is reversed (backward propagation), light travels through an adiabatic downtaper and thus one fiber mode is incident on the microresonator. Although the uptaper is non-adiabatic and couples some light from each fiber waist mode into the single-mode untapered

fiber, switching the direction of propagation of light through an asymmetric tapered fiber offers a rough way to compare experimental with theoretical enhancement.

5. EXPERIMENTAL RESULTS

A typical experimental setup is shown in Fig. 4. A thin-walled HBR with a wall thickness of 5-10 μm is made and is glued to an HBR stand. The light from a tunable diode laser (1508-1585 nm) is frequency scanned using a function generator (FG). The beam travels through an anamorphic prism (AP), an optical isolator (OI), a set of waveplates (WP), the fiber coupler (FC), and an optical fiber isolator before reaching the tapered fiber. The waveplates control the input polarization of the light whereas the fiber isolator reduces the Fabry-Perot fringes due to reflections from the fiber ends.

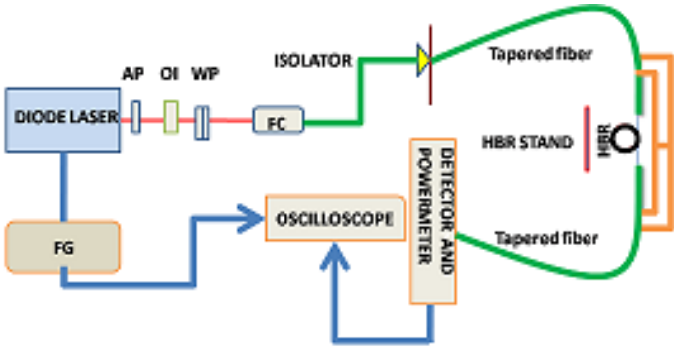

Fig. 4. Experimental setup used for dye sensing.

An asymmetric tapered fiber with a non-adiabatic downtaper and an adiabatic uptaper is used to couple light into and out of the microresonator. After the light from the non-adiabatic tapered fiber is coupled into a resonator filled with methanol, analyte (dye) at predetermined concentrations was added to the methanol and changes in WGM dip depths were recorded at $\beta = 0$. Then the direction of propagation of light is switched by swapping the ends of the tapered fiber and changes in WGM dip depth with different analyte concentrations were recorded and processed. The throughput spectra corresponding to different propagation directions are shown in Fig. 5.

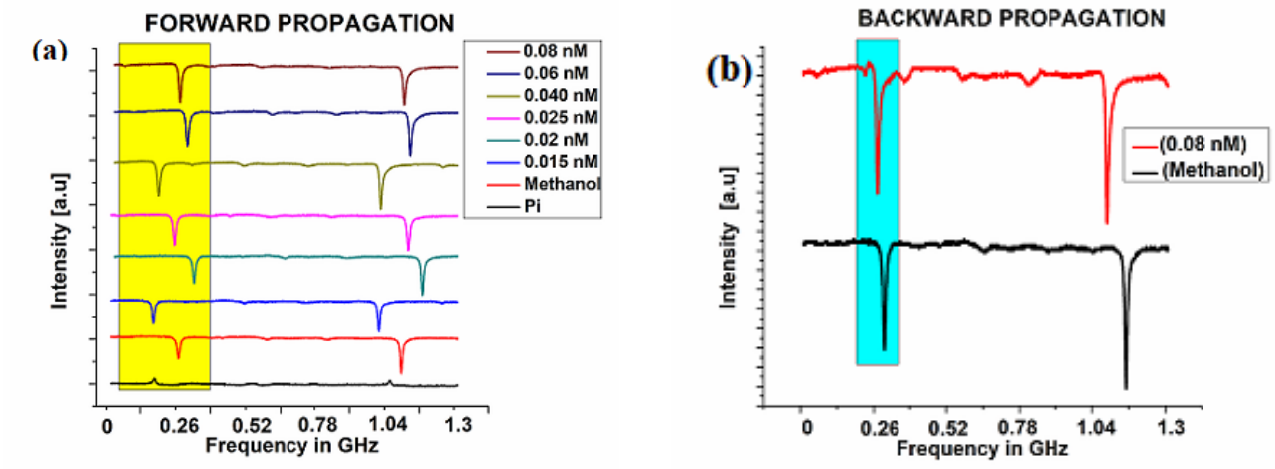

Fig. 5. Throughput spectra corresponding to different analyte concentrations. Upward shift indicates increasing analyte concentration. (a) Forward propagation; bottom trace for methanol only, $\beta = \pi$. (b) Backward propagation.

For backward propagation, the change in dip depth is very small, even at the high concentration in Fig. 5, and hence the uncertainty in measuring the fractional change in dip depth is almost twice the fractional change in dip depth itself. The

experimental fractional change in dip depth $\frac{dM}{M}$ is assumed to be linear and is found at lower concentrations by extrapolating the dip depth measured at high concentration. A summary of the experimental analysis is given in Table 1 for the mode highlighted in Fig. 5. Using the value of absorption coefficient of analyte α_a, the internal evanescent fraction f of the WGM was determined to be 0.25 by fitting multiple dip depths for various analyte concentrations. The percent deviation of the experimental dip depth from the theoretical dip depth suggests that the preliminary results match well with the model. However, the discrepancy between experimental and theoretical enhancement can be attributed to the fact that the experiment, for reverse propagation, is not as simple as the model assumes. When light propagates in the reverse direction, the outcoupled light from the microresonator travels through a non-adibatic uptaper which results in coupling between the fundamental and higher-order fiber modes, and hence a modified dip is seen in the observed spectrum. Furthermore, for reverse propagation, the change in observed dip depth is so small that any measurment will have a very significant uncertanity.

Table 1. Summary of results for dye sensing, $f = 0.25$.

Dye concentration in nM	Experimental dip depth	Theoretical dip depth	Deviation of experimental from theoretical dip depth	Experimental enhancement	Theoretical enhancement
Methanol	0.0949 ± 0.0011	0.0905	4.8%		-
0.015	0.1032 ± 0.0016	0.1039	0.5%	50 (+100/-50)	1112 ± 67
0.040	0.1246 ± 0.0009	0.1172	6.3%	67 (+134/-67)	831 ± 50
0.08	0.1400 ± 0.0001	0.1385	1.0%	51 (+102/-51)	747 ± 37

An experimental setup similar to that shown in Fig. 4 is used for trace gas (carbon dioxide) sensing. A low-pressure reference cell is used for identifying the CO_2 absorption lines. The microresonator is attached to a piezo stretcher which strain-tunes the WGMs on and off resonance with respect to the trace gas absorption line. An experimental procedure similar to that used for dye sensing was followed, and the throughput spectrum corresponding to different propagation directions was recorded and processed as shown in Fig. 6.

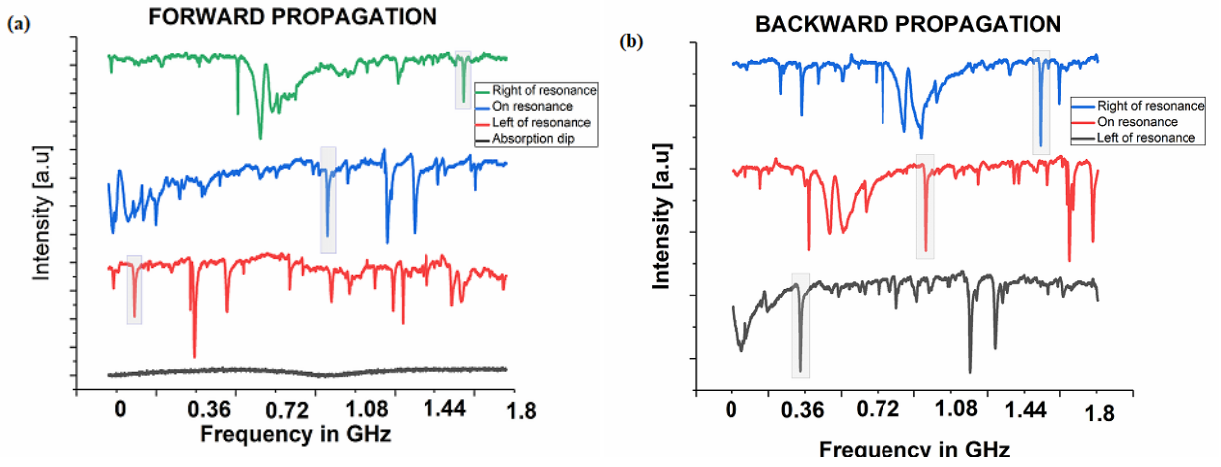

Fig. 6. Traces showing WGM affected by CO_2 absorption lines around 1572 nm in 5% mixture in air at atmospheric pressure. (a) Forward propagation. (b) Backward propagation.

In Fig. 6(a), the black trace indicates the CO_2 absorption dip seen in the reference cell transmission whereas red, blue, and green traces indicate the change in dip depth when the highlighted WGM is left of resonance, on resonance, and

right of resonance, respectively. An analysis similar to that shown in Table 1 was done. The theoretical enhancement factor was 152 ± 9, and the experimental enhancement factor was found to be 14 (+140/-14).

6. DISCUSSIONS

This work demonstrates an enhancement in chemical absorption sensitivity when a non-adiabatic tapered fiber is used instead of an adiabatically tapered fiber to couple light into a microresonator. For the forward propagation case, the experimental dip depth is in good agreement with the theoretical dip depth predicted by the model, showing that the internal evanescent fraction *f* of this mode was 0.25. This tells us that the model is reliable and that this WGM is one of fairly high radial order. Even though there is a large uncertainty in the experimental sensing enhancement, the enhancement is evident from the throughput spectra shown in Figs. 5 and 6. A better comparison of the results of forward and reverse propagation, and hence between experimental and theoretical enhancement, will be given by a new model that is currently under development.

REFERENCES

[1] Foreman, M. R., Swaim, J. D., and Vollmer, F., "Whispering gallery mode sensors," Adv. Opt. Photon. 7, 168-240 (2015).

[2] Rosenberger, A. T., "Analysis of whispering-gallery microcavity-enhanced chemical absorption sensors," Opt. Express 15, 12959-12964 (2007).

[3] Farca, G., Shopova, S. I., and Rosenberger, A. T., "Cavity-enhanced laser absorption spectroscopy using microresonator whispering-gallery modes," Opt. Express 15, 17443-17448 (2007).

[4] Ward, J. M., Dhasmana, N., and Nic Chormaic, S., "Hollow core, whispering gallery resonator sensors," Eur. Phys. J. Spec. Top. 223, 1917–1935 (2014).

[5] Murugan, G. S., Petrovich, M. N., Jung, Y., Wilkinson, J. S., and Zervas, M. N., "Hollow-bottle optical microresonators," Opt. Express 19, 20773-20784 (2011).

[6] Stoian, R.-I., Bui, K. V., Rosenberger, A. T., "Silica hollow bottle resonators for use as whispering gallery mode based chemical sensors," J. Opt. 17, 125011 (2015).

[7] Rosenberger, A. T., "Absorption sensing enhancement in a microresonator coupled to a non-adiabatic tapered fiber," Proc. SPIE 10548, 105480G (2018).

[8] Birks, T. A., and Li, Y. W., "The Shape of Fiber Tapers," J. Lightwave Technol. 10, 432-438 (1992).

[9] Zibaii, M. I., Latifi, H., Karami, M., Gholami, M., Hosseini, S. M., and Ghezelayagh, M. H., "Non-adiabatic tapered optical fiber sensor for measuring the interaction between α-amino acids in aqueous carbohydrate solution," Meas. Sci. Technol. 21**,** 105801 (2010).

[10] Latifi, H., Zibaii, M. I., Hosseini, S. M., and Jorge, P., "Nonadiabatic Tapered Optical Fiber for Biosensor Applications," Photonic Sensors 2, 340–356 (2012).

[11] Muhammad, M. Z., Jasim, A. A., Ahmad, H., Arof, H., and Harun, S. W., "Non-adiabatic silica microfiber for strain and temperature sensors," Sensors and Actuators A 192, 130-132 (2013).

[12] Luo, L., Pu, S., Tang, J., Zeng, X., and Lahoubi, M., "Reflective all-fiber magnetic field sensor based on microfiber and magnetic fluid," Opt. Express 23, 18133-18142 (2015).

[13] Zhang, K., Wang, Y., and Wu, Y.-H., "Enhanced Fano resonance in a non-adiabatic tapered fiber coupled with a microresonator," Opt. Express 42, 2956-2959 (2017).